

Light scattering by horizontally oriented ice plates.

II. Scattering matrix

A.V. Burnashov and A.G. Borovoi

*Institute of Atmospheric Optics,
Siberian Branch of the Russian Academy of Sciences, Tomsk*

Received April 18, 2007

Basic qualitative regularities for all elements of the scattering matrix are considered in the case of scattering by hexagonal ice plates oriented in the horizontal plane. For parhelic and subparhelic circles, it is shown that polarization of light scattered in the angles from sundog to 120° parhelic is similar to that of incident light. A method is proposed for diagnostics of ice plate thickness from ground-based polarization measurements within sundog with the use of a laser source with circularly polarized light.

1. Scattering matrix

In the general case, light polarization is determined by three real parameters. In particular, the Stokes vector parameters $\mathbf{I} = (I, Q, U, V)$, where I is the intensity, and Q and U determine the linear polarization, while V determines the circular polarization, are used most widely. In the previous paper,¹ we have considered only the intensity I of the light scattered at horizontally oriented ice plates and in the case of the fully nonpolarized incident light ($Q = U = V = 0$). In this paper, we consider all polarization characteristics of the scattered light at the arbitrary polarization of the incident light.

In the problem of light scattering by an isolated particle, the light $\mathbf{I}(\mathbf{n})$ scattered in the direction \mathbf{n} is related to the incident light $\mathbf{I}_0(\mathbf{n}_0)$ through the matrix \mathbf{Z} :

$$\mathbf{I}(\mathbf{n}) = \mathbf{Z}(\mathbf{n}, \mathbf{n}_0) \mathbf{I}_0(\mathbf{n}_0). \quad (1)$$

Equation (1) should be complemented with determination of two arbitrary coordinate systems, in which the vectors $\mathbf{I}(\mathbf{n})$ and $\mathbf{I}_0(\mathbf{n}_0)$ are specified. Currently, in scattering theory a commonly accepted terminology for the matrix \mathbf{Z} is absent. Thus, if both coordinate systems are fixed, then \mathbf{Z} is referred to in the international literature as a *phase matrix*² or *Mueller matrix*,³ whereas the term *scattering matrix* is used for the matrix related to the scattering plane, that is, to the plane drawn through the vectors \mathbf{n} and \mathbf{n}_0 . Following Ref. 4, we call \mathbf{Z} the scattering matrix.

In the case of light scattering by horizontally oriented particles, it is convenient to use the coordinate system determined in the following way. At the sphere of scattering directions \mathbf{n} , select two polar points corresponding to scattering in the forward $\theta = 0$ and backward $\theta = \pi$ directions. Then the zero meridian $\varphi = 0$ is selected arbitrarily, and the azimuth angle is measured clockwise from this meridian as viewed from the center of the sphere in

the direction of the forward scattering. Then for every direction of scattering $\mathbf{n} = (\theta, \varphi)$, in the plane tangent to the sphere it is possible to define uniquely the unit zenith \mathbf{e}_θ and azimuth \mathbf{e}_φ vectors directed toward the increase of the zenith θ and azimuth φ angles. Three vectors \mathbf{n} , \mathbf{e}_θ , and \mathbf{e}_φ form the right-hand set of vectors according to the relation $\mathbf{n} = \mathbf{e}_\theta \times \mathbf{e}_\varphi$. These vectors form the basis for representation of the scattered electric field in the form of the zenith $E_\theta(\theta, \varphi)$ and azimuth $E_\varphi(\theta, \varphi)$ components. The Stokes parameters in this basis can be determined as²:

$$I = |E_\theta|^2 + |E_\varphi|^2; \quad Q = |E_\theta|^2 - |E_\varphi|^2; \\ U = -(E_\theta E_\varphi^* + E_\varphi E_\theta^*); \quad V = -i(E_\theta E_\varphi^* - E_\varphi E_\theta^*). \quad (2)$$

It should be noted that the usual³⁻⁵ definition of U and V differs from Eqs. (2) by the opposite sign, but the numerical values of the Stokes parameters coincide, since the basis vector \mathbf{e}_φ in Refs. 3-5 has the opposite direction. Now consider the incident light $\mathbf{I}_0(\mathbf{n}_0)$. The direction of propagation of the incident light \mathbf{n}_0 can be shown in the sphere of scattering directions as a vector directed from the point $\mathbf{n}_0 = (\theta_0, \varphi_0)$ to the sphere center. Then the Stokes parameters \mathbf{I}_0 are determined similarly to those for the scattered field, but with the vector \mathbf{e}_θ replaced with the vector $(-\mathbf{e}_\theta)$ in order to preserve the right-hand system of the basis vectors for the light propagating in an arbitrary direction.

The scattering matrix fully determines all light scattering properties of a particle with accounting for any states of polarization of the incident light. This matrix is convenient for numerical calculations, but physical meaning of its components Z_{ij} is not clear, that complicates their interpretation. Therefore, we use another equivalent matrix, whose physical meaning is more obvious. For this purpose, we divide the initial scattering matrix into a set of four columns, which can be interpreted as some four Stokes vector parameters $\mathbf{Z}_{ij} = (Z_{1j}, Z_{2j}, Z_{3j}, Z_{4j}) = (\mathbf{Z}_1, \mathbf{Z}_2, \mathbf{Z}_3, \mathbf{Z}_4)$. Then

we form a new equivalent matrix Y_{ij} through constructing four new columns by the following rule:

$$\begin{aligned} \mathbf{Y}_1 &= \mathbf{Z}_1, \mathbf{Y}_2 = \mathbf{Z}_1 + \mathbf{Z}_2, \\ \mathbf{Y}_3 &= \mathbf{Z}_1 + \mathbf{Z}_3, \mathbf{Y}_4 = \mathbf{Z}_1 + \mathbf{Z}_4. \end{aligned} \quad (3)$$

Then the columns \mathbf{Y}_i have the meaning of the Stokes parameters at the incident light with unit intensity. In particular, \mathbf{Y}_1 corresponds to fully nonpolarized light ($I_0 = 1, Q_0 = U_0 = V_0 = 0$), while three other columns $\mathbf{Y}_2, \mathbf{Y}_3$, and \mathbf{Y}_4 correspond to fully polarized light. Here \mathbf{Y}_2 corresponds to the linear polarization along the vector \mathbf{e}_0 ($I_0 = Q_0 = 1, U_0 = V_0 = 0$), \mathbf{Y}_3 stands for the linear polarization at an angle of 45° ($I_0 = U_0 = 1, Q_0 = V_0 = 0$), and \mathbf{Y}_4 is for the circular polarization in the incident light ($I_0 = V_0 = 1, Q_0 = U_0 = 0$). Thus, all elements of the matrix Y_{ij} have a simple physical meaning and can be measured directly in the experiment. Usually, the elements of the matrix Z_{ij} presented in the literature are normalized to the first element of the first column, that is, $Z'_{ij} = Z_{ij}/Z_{11}$. In our new matrix, to preserve the above physical interpretation, we normalize the second, third, and fourth elements of each column to the first element of this column, that is,

$$M_{ij} = Y_{ij}/Y_{1j}. \quad (4)$$

Then the first element in the j -th column of \mathbf{M} is the intensity of light scattered in the direction \mathbf{n} at the given polarization of the incident light, while three other dimensionless elements determine the polarization of the scattered light. In particular, the degrees of the linear p_j^l and circular p_j^c polarizations used in practice are determined by the equations

$$p_j^l = \sqrt{M_{2j}^2 + M_{3j}^2}, \quad p_j^c = |M_{4j}|. \quad (5)$$

The normalized matrix \mathbf{M} determined by Eq. (4) is an object of our calculations. Certainly, at the known scattering matrix \mathbf{M} , it is easily to pass to the traditional scattering matrix \mathbf{Z} through the linear transformation, inverse to Eqs. (3).

Note some features of calculation of scattering matrices. It is obvious that within the framework of the geometric-optics approximation, the scattered light near the crystal surface is a superposition of plane-parallel beams. Each beam is characterized by its own trajectory of photons, that is, a sequence of collisions with certain crystal sides. Correspondingly, it is natural to calculate the scattering matrix as a sum of scattering matrices for all beams calculated by the well-known geometric-optics algorithms. However, this procedure calls for some explanations. For this purpose, we consider first the light scattering at a crystal with fixed orientation.

For different trajectories of photons, the scattering directions usually differ. However, there are sets of "related" trajectories (or beams) having the same scattering direction. For example, any parallel crystal sides form sets of related trajectories, which are well-known for plane-parallel plates.⁵ As it is known, at fully polarized incident field and at a

fixed orientation of a particle, the scattered field should be fully polarized as well. Therefore, we should sum up the contribution from related trajectories at a level of 2×2 Johns matrices, rather than \mathbf{Z} or \mathbf{Y} (note that the non-normalized 4×4 matrices should be summed). In other words, in terms of 4×4 scattering matrices, we should sum both the scattering matrices themselves, obtained for different trajectories, and the matrices determining the interference between corresponding fields. However, if the phase incursions for trajectories differ significantly, the interference between the scattered light beams can be neglected. Actually, in this case the interference terms give, on average, zero for statistical ensembles with a crystal size spread. Therefore, we directly summarize the 4×4 scattering matrices for related photon trajectories. Since non-related trajectories at a fixed orientation of a crystal give different scattering directions, the interference does not appear for them. Therefore, in statistical averaging of the scattering matrix over crystal orientations, the summation of 4×4 scattering matrices for non-related trajectories is a physically rigorous procedure. However, for related trajectories, such summation is true accurate to interference terms.

2. Scattered light polarization at polarized and nonpolarized incident light

Our task is to calculate the scattering matrix for a horizontally oriented hexagonal ice plate at statistical averaging over the angles of plate rotation about the vertical axis. In the previous paper,¹ we have considered in detail the intensity of the light scattered along three main scattering circles. The data obtained were represented as a set of plots at several fixed values of both zenith angle of light incidence θ_0 and the shape parameter of the plate $F = h/2H$ (in the international literature, the parameters F , in which h is the plate thickness and H is the length of hexahedron side, is referred to as an *aspect ratio*). Due to the limited volume of this paper, it is impossible to present all analogous plots for the scattering matrix. Therefore, we consider main qualitative regularities obtained for scattering matrices for the parhelic and subparhelic circles at the light incidence angle $\theta_0 = 75^\circ$ and the shape parameter $F = 0.4$ taken as an example. The plots obtained for elements of the scattering matrix $M_{ij}(\varphi)$ are shown in Fig. 1.

Note that all elements of the matrix $M_{ij}(\varphi)$ are shown in Fig. 1 for the range of scattering angles $[0-180^\circ]$. In the remaining range $[180-360^\circ]$, the elements of the scattering matrix for the first two columns are determined by the symmetry $M_{ij}(\varphi) = M_{ij}(360^\circ - \varphi)$ (for elements $M_{11}, M_{21}, M_{12}, M_{22}$) or antisymmetry $M_{ij}(\varphi) = -M_{ij}(360^\circ - \varphi)$ (for elements $M_{31}, M_{41}, M_{32}, M_{42}$). For the third and fourth columns, these relations are not fulfilled, but they are true for all columns of the initial matrix Z of

Eq. (1) [Ref. 9], which allows other elements of the matrix $M_{ij}(\varphi)$ to be easily constructed in the range $[180-360^\circ]$.

As is seen from Fig. 1, the scattered light intensities in the parhelic and subparhelic circles include singularities and sharp peaks, considered in

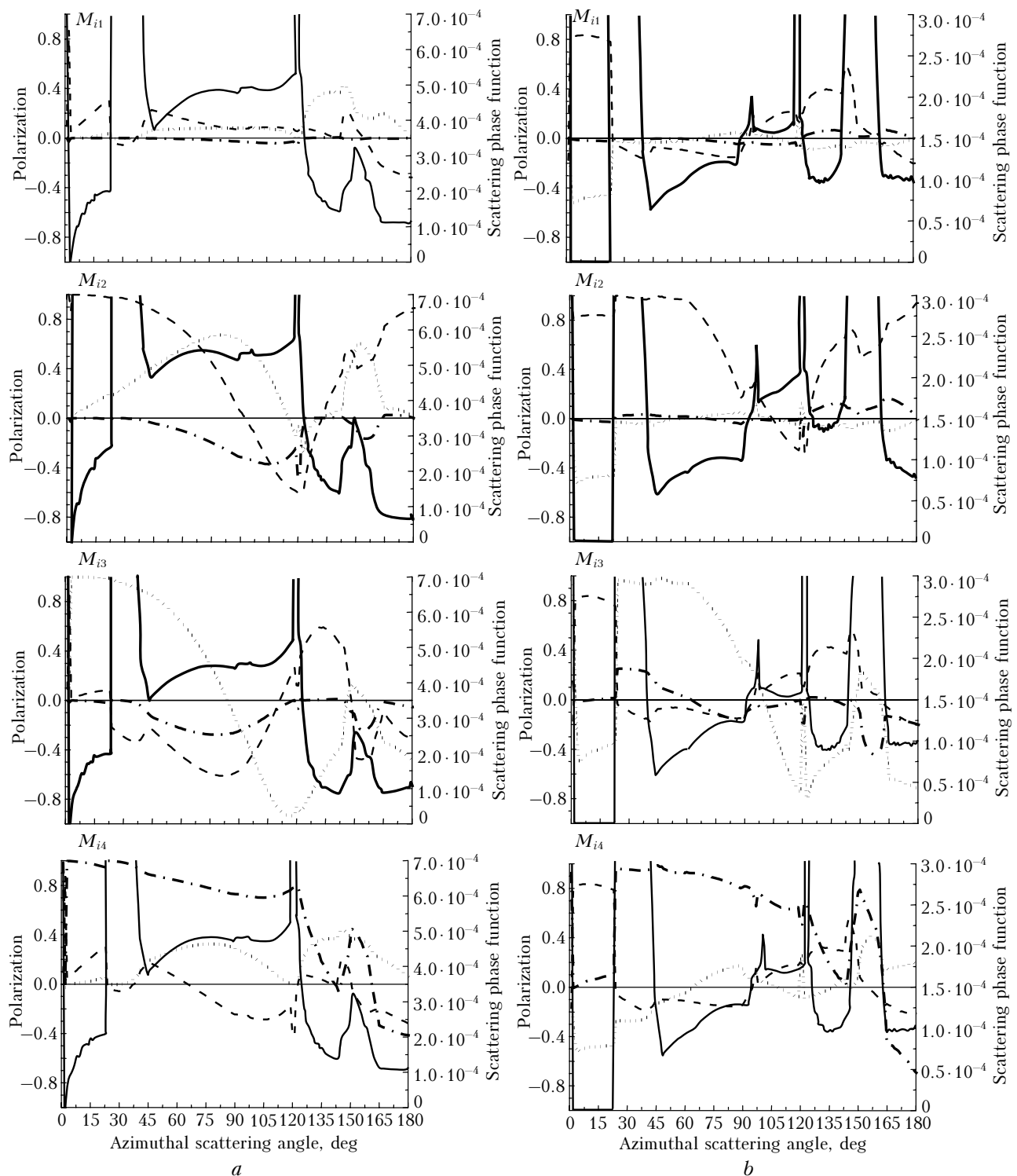


Fig. 1. Scattering matrix $M_{ij}(\varphi)$ of a hexagonal plate for parhelic (*a*) and subparhelic (*b*) circles: intensity of scattered light I (solid curve), component Q linearly polarized at an angle of 0° (dashed curve), component U linearly polarized at an angle of 45° (dots), circularly polarized component V (dot and dash curve). The right ordinate plots the intensity, while the left one shows polarization; fully nonpolarized incident light (first row), light linearly polarized at an angle of 0° (second row), light linearly polarized at an angle of 45° (third row), and circularly polarized incident light (fourth row).

detail in Ref. 1, whereas other elements of the scattering matrix, describing polarization, appear to be rather smooth functions. The variety of the circles $M_{ij}(\varphi)$, where $i \geq 2$, can be easily interpreted based on the following two physical facts. First, our calculations have shown that the number of scattered beams contributing significantly to this scattering angle is small: about three. The photon trajectories characterizing each beam have no more than three collisions. Second, it is obvious that the greater is the number of collisions in a given photon trajectory, the stronger, on average, the degree of polarization in the scattered beam differs from the polarization of the incident radiation and, to the contrary, the smaller is the cross section of the scattered beam, that is, the smaller is its contribution to the total intensity of the scattered light.

Let us divide the scattering angles into several characteristic intervals and begin the consideration from the interval of angles for the sundog peak. Here, as was already mentioned,¹ the major contributor is the trajectory with two collisions, when a photon passes through a dihedral angle of 60°. Then, between the sundog region and 120° parhelion, the analogous trajectory with three collisions, in which a photon additionally collides with a vertical side, becomes dominating. Trajectories with a large number of collisions contribute to large scattering angles [120–180°]. As it was seen earlier,¹ when discussing the peak at 150°, such trajectories contribute to their own narrow ranges of scattering angles, which often do not overlap.

The above physical reasoning allows the form of the functions $M_{ij}(\varphi)$, where $i \geq 2$, to be easily interpreted. Start the discussion from the case of fully nonpolarized incident light for the parhelic and subparhelic circles. As can be seen from the first row of Fig. 1, the elements of the scattering matrix M_{21} , M_{31} , and M_{41} are small here, starting from the sundog peak and to 120° parhelion. This is explained by the fact that the number of photon collisions in trajectories contributing significantly to this range of angles is small. As a result, the polarization of the scattered light only slightly differs from the polarization of the incident radiation. In the angular range 120–180°, the degree of polarization somewhat increases and oscillates. However, the maximum of polarization often falls on the minimum of intensity, which is characteristic of photon trajectories with a large number of collisions. That is why such polarization can be hardly observed experimentally.

It remains for us to consider the angular range between the direction of forward scattering and sundog. Here, in parhelic circle, relatively low intensity of the scattered light results from the trivial single light reflection from vertical crystal sides. In the subparhelic circle, such a trajectory does not exist, and this interval of scattering angles is filled due to some trajectory with 6 collisions, which is omitted here for brevity. Although the polarization in this beam sharply increases due to the large number

of collisions, the area of the beam leads to the negligibly low scattered light intensity. Therefore, the so strong polarization in the subparhelic circle in the angular range 0–22° is of no practical interest.

Thus, we can draw the following general conclusion: when horizontally oriented ice plates are irradiated by nonpolarized light, the degree of polarization in the scattered light is low and the polarization measurements in this case show no promises from the viewpoint of obtaining information about crystal parameters.

Now we pass on to the irradiation of plates by fully polarized light, that is, to elements of the scattering matrix $M_{ij}(\varphi)$, where $i, j \geq 2$. At fully polarized incident light, the following regularities should be observed for the scattered light. First, if only one trajectory significantly contributes to the given scattering angle, then the scattered light also should be fully polarized, that is, the degree of polarization P_j is equal to unity:

$$P_j = \sqrt{(p_j^1)^2 + (p_j^2)^2} = 1. \quad (6)$$

If we have a sum of contributions from beams with different trajectories, then the degree of polarization decreases: $P_j < 1$. Thus, from the experimentally measured degree of polarization of the scattered light we can extract the information about the number of photon trajectories, efficiently contributing to this direction of scattering.

Second, the degree of polarization can sometimes reach zero, that is, we obtain fully nonpolarized scattered light at fully polarized incident light. In particular, scattered light in Fig. 1 is fully nonpolarized in the parhelic circle at the scattering angle $\varphi \approx 133^\circ$ with incident light polarized linearly at an angle of 0°. To illustrate this fact, Figure 2 shows that three trajectories contribute significantly to this scattering angle. Trajectory 1 corresponds to the trivial reflection from the vertical side. In trajectory 2, the light enters through the horizontal side, reflects from the vertical side, and exits through the opposite horizontal side. In trajectory 3, the light enters through one vertical side, reflects from the other, and exits through the third vertical side. Figure 2 shows the element of the matrix $M_{22}(\varphi)$ for each trajectory and for total radiation. As follows from Fig. 2, here the elements with the same signs of the non-normalized scattering matrix $Y_{22}(\varphi)$ [see Eq. (3)] for trajectories 1 and 3 are summarized, whereas for trajectory 2 the signs are opposite, which gives zero in sum. Analogously, as follows from Fig. 1, other two elements M_{32} and M_{42} also vanish in the total radiation at a scattering angle of 133°.

As to the qualitative behavior of $M_{ij}(\varphi)$, where $i, j \geq 2$, it is similar to the case of fully nonpolarized incident light, which was considered above. Namely, in the region of the sundog peak, the polarization of the scattered light differs only slightly from the polarization of the incident radiation. Then, in the angular range up to 120°, the polarization varies

smoothly, which corresponds to the predominant trajectory with three collisions mentioned above. In the angular range 120–180°, the matrix elements oscillate due to superposition of trajectories with a large number of collisions.

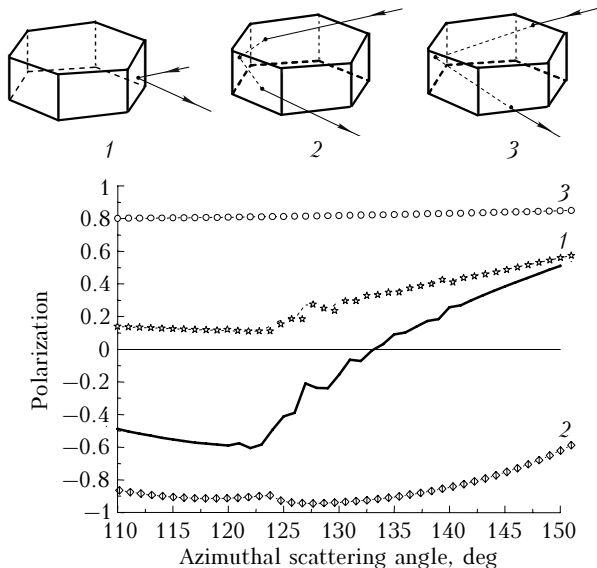


Fig. 2. Three trajectories contributing significantly near the scattering angle $\varphi = 133^\circ$. Figure shows the element of the scattering matrix $M_{22}(\varphi)$ for each trajectory and (solid curve) the element $M_{22}(\varphi)$ for the total radiation.

3. Determination of the plate shape parameter from polarization measurements of scattered light

Let us consider the problem of light scattering at ice plates, chaotically oriented in the horizontal plane from the viewpoint of inverse problems, that is, from the viewpoint of reconstruction of particle parameters from the radiation scattered by the particles. As was shown in the previous section, the polarization of the scattered light at the nonpolarized sensing radiation is insignificant. Therefore, the ground-based polarization measurements, for example, in the parhelic circle appearing as the sunlight passes through cirrus clouds, are not promising. For polarization measurements of the scattered radiation, a source of polarized radiation (laser) is necessary.

By now there appear much literature, where backscattering radiation of lidar signals is used for polarization diagnostics of cirrus clouds.^{6–8} At the same time, the backscattered light, first, has low intensity and, second, carries less information as compared to other scattering directions. In this section we consider a possibility of reconstructing the shape parameters F of plates from polarization measurements at the optimally selected incidence and scattering angles. If a ground-based laser source of radiation is used for diagnostics of crystalline particles in the atmosphere, then the scattered light recorded on the ground corresponds to the subparhelic circle.

Assume that for ice plates existing in the atmosphere the shape parameters $F = h/2H$ lie in the range [0.1–0.4]. Consequently, we have to select the optimal values of the incidence and scattering angles for the subparhelic circle, in which the elements of the $M_{ij}(\varphi)$ at $i, j \geq 2$ are most sensitive to variations of F in the given range. In the subparhelic circle, the main part of the scattered light is concentrated in four narrow peaks, among which the main peaks are sundog and the peak of forward scattering corresponding to the mirror-reflected component of the scattered light. Just these peaks are considered in this section from the viewpoint of scattering inverse problems.

The formulation of such inverse problem is based on the following physical reasoning. In general case, if the given photon trajectory includes no events of total internal reflection, then the linearly polarized incident light is transformed into the scattered light, which is also linearly polarized. The component with circular polarization can appear in this case only due to total internal reflection, which appears at hexagonal sides of a plate at incidence angles $\pi/2 - \theta^* < \theta_0 < \theta^*$, where $\theta^* \approx 58^\circ$ [Ref. 1]. It can be easily found from geometric consideration that at $F = 0.4$ and the incidence angle $\theta_0 \approx 34^\circ$ the trajectory with only one total internal reflection takes place. In this case, the light enters through a crystal lateral side, reflects from its hexagonal side, and exits through another lateral side at the third collision. Then, as F decreases, the trajectories with three, five, and more total internal reflections at horizontal sides appear and become predominate.

Thus, the scattered component with the circular polarization increases stepwise with F decrease. Just this dependence can be used for diagnostics of the plate shape. This qualitative reasoning was checked and implemented in our calculations.

Figure 3 depicts the elements of the scattering matrix in sundog (near its left sharp edge) at variation of a plate shape parameter $M_{ij}(F)$ for incident light with linear and circular polarizations.

We can see the two-stage character of the curves in all the plots, where one stage in the region of $F = 0.4$ corresponds to the trajectory with one total internal reflection, while another in the region of $F \approx 0.2$ corresponds to the prevailing contribution from the trajectory with three total internal reflections. The linear and the steepest function $M_{ij}(F)$ is optimal for the problem of reconstruction of a plate shape parameter from the experimentally measured element of the scattering matrix. The element $M_{44}(F)$ best corresponds to this criterion.

Thus, the following scheme can be proposed for the polarization diagnostics of the shape parameter F . The incident radiation should be circularly polarized, and the component with the circular polarization should be detected in the scattered light. The range of incidence angles in this case should be narrow, within 34–36°, since as it is seen from Fig. 3, starting from the scattering angles $\theta_0 \approx 36^\circ$, the quasilinear character of the functions $M_{ij}(F)$ is broken.

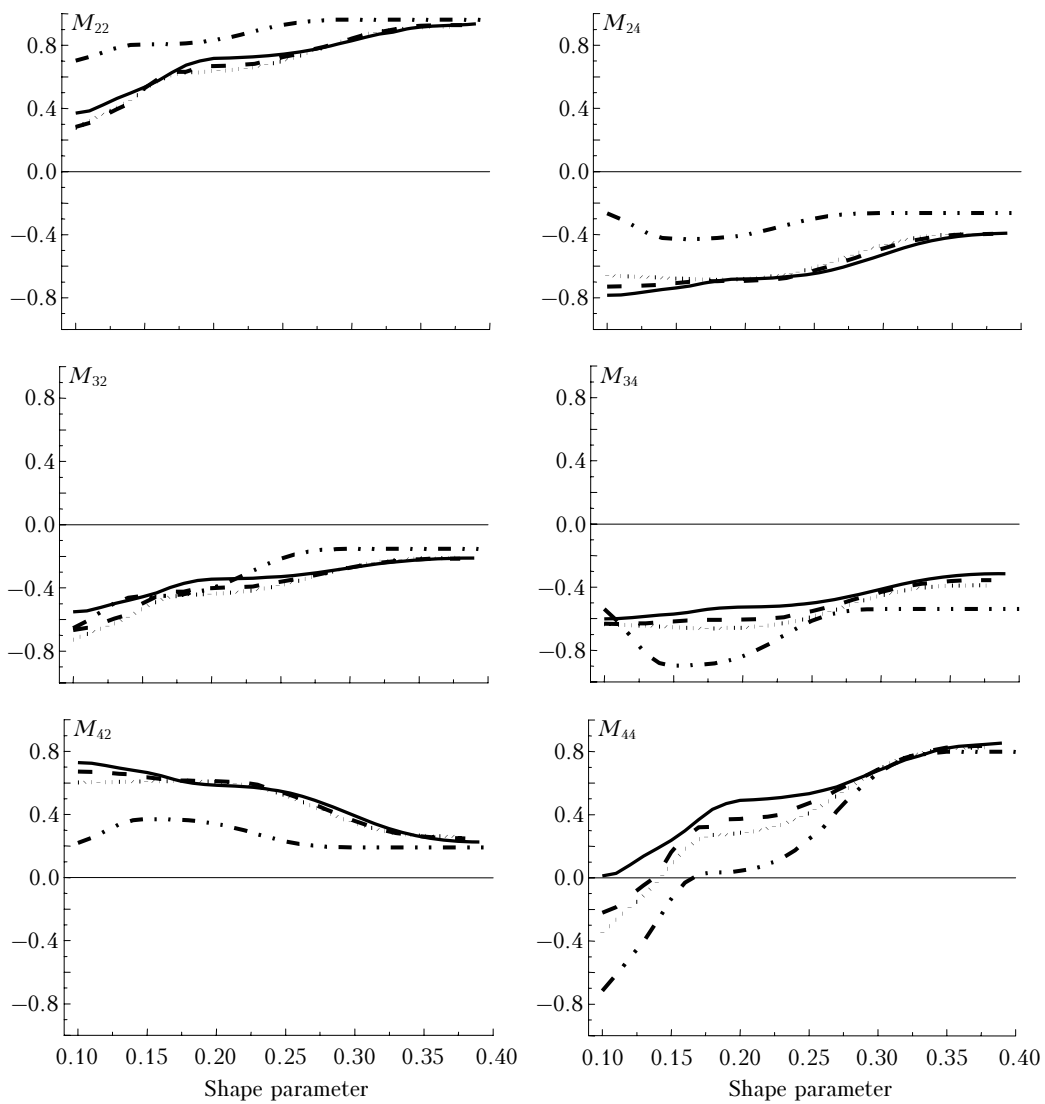


Fig. 3. Polarization in sundog as a function of the shape parameter of a plate; the left column corresponds to the radiation linearly polarized at an angle of 0° , and the right column corresponds to the circularly polarized radiation: zenith angle of incidence $\theta_0 = 34^\circ$ (solid curve), 35° (dashed curve), 36° (dotted curve), and 42° (dash-and-dot curve).

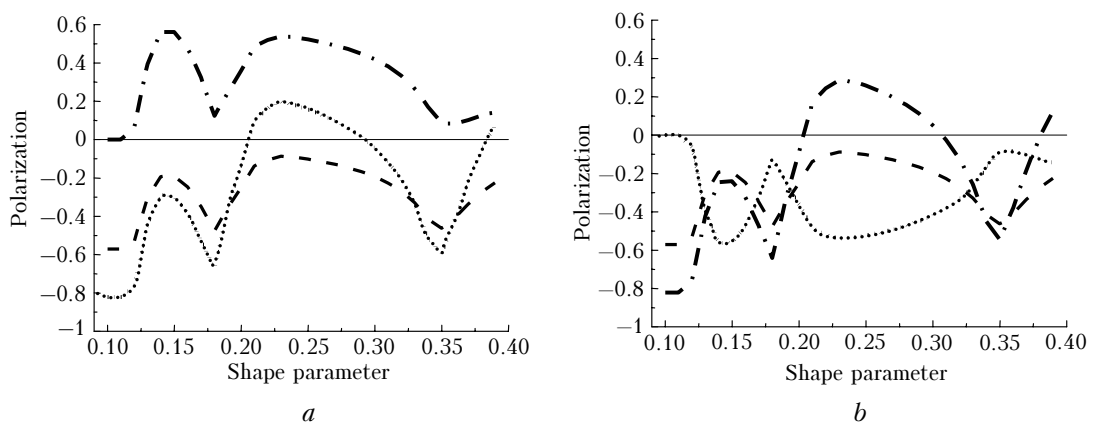


Fig. 4. Polarization at the peak of forward scattering as a function of the shape parameter of a plate for the incident radiation linearly polarized at an angle of 45° (a) and circularly polarized (b); incidence angle of 34° ; M_{23} and M_{24} elements of the scattering matrix (dashed curves), M_{33} and M_{34} (dotted curves), and M_{43} and M_{44} (dash-and-dot curves).

The analogous quasilinear character of $M_{ij}(F)$ due to trajectories with total internal reflection from horizontal sides could be also expected in the peak of forward scattering. However, in this case these trajectories are supplemented with the trajectories, in which photons either directly reflect from the horizontal side or enter a plate through the horizontal, rather than vertical, side. Figure 4 demonstrates that the contribution of these trajectories distorts the quasilinear dependence of $M_{ij}(F)$ and the peak of forward scattering appears to be unpromising from the viewpoint of F reconstruction from polarization measurements.

Acknowledgements

This work was supported in part by the Russian Foundation for Basic Research (Grants Nos. 05–05–39014 and 06–05–65141) and INTAS (Grant No. 05–1000008–8024).

References

1. A.V. Burnashov and A.G. Borovoi, *Atmos. Oceanic Opt.* **20**, No. 7, 534–542 (2007).
2. M.I. Mishchenko, L.D. Travis, and A.A. Lacis, *Scattering, Absorption, and Emission of Light by Small Particles* (Cambridge University Press, Cambridge, 2002), 445 pp.
3. A.A. Kokhanovsky, *Polarization Optics of Random Media* (Praxis-Springer, Chichester, 2004), 224 pp.
4. C.F. Bohren and D. Huffman, *Absorption and Scattering of Light by Small Particles* (John Wiley, New York 1983).
5. M. Born and E. Wolf, *Principles of Optics* (Pergamon, New York, 1959).
6. B.V. Kaul', S.N. Volkov, and I.V. Samokhvalov, *Atmos. Oceanic Opt.* **16**, No. 4, 325–332 (2003).
7. B.V. Kaul, I.V. Samokhvalov, and S.N. Volkov, *Appl. Opt.* **43**, 6620–6628 (2004).
8. V. Noel and K. Sassen, in: *Proc. of 22th Int. Laser Radar Conference (ILRC 2004)* (ESA, Matera, Italy, 2004), pp. 309–312.
9. V. Noel, G. Ledanois, H. Chepfer, and P.H. Flamant, *Appl. Opt.* **40**, 4365–4375 (2001).